Influence of Surface Excitations on Quantitative Analysis in Electron Spectroscopy

Yung-Fu Chen

Precision Instrument Development Center, National Science Council, Hsinchu, Taiwan, R.O.C

(Received October 5 1998; accepted January 13 1999)

The inelastic interaction of electrons with solid surfaces is studied within the framework of dielectric response theory. It is shown that the inelastic scattering can be characterized by the differential inverse inelastic mean free path (DIIMFP) for bulk excitations and the differential surface excitation parameter (DSEP) for surface effects. With the derived bulk DIIMFP and DSEP, the influence of surface excitations on quantitative analysis in surface electron spectroscopies is investigated. The discussions include background removal in surface electron spectroscopies and angular distribution of photoelectrons emitted from solids

1. INTRODUCTION

Tougaard and coworkers [1-3] have pioneered the application of reflection electron energy loss spectroscopy (REELS) experiments to gain knowledge about inelastic scattering cross sections, $K(E_o \to E_o - \omega)$. Here E_o is the incident electron energy and ω is the electron-energy loss. The experimentally determined $K(E_o \to E_o - \omega)$ are significantly different from the conventional DIIMFP for bulk excitations due to the surface effects [3-5]. The method of Tougaard and Chorkendorff becomes especially attractive because the determined DIIMFP may be applied to remove the inelastic background signal from AES or XPS spectra [1,2,6,7]. However, an inherent problem is that $K(E_o \to E_o - \omega)$ determined from REELS data contain information associated with electrons traversing the solid-vacuum surface twice while, in the AES or XPS measurement, the signal electrons traverse this surface only once. As a result, the intensities associated with the surface excitations in REELS spectra are enhanced with respect to the AES or XPS measurement [8,9].

In this work, we used dielectric response theory to derive the DIIMFP for electrons obliquely passing through the solid surface. It was found that the derived DIIMFP can be divided into a bulk and a surface term. The bulk term is the DIIMFP in an infinite medium, while the surface term is spatially varying on both sides of the vacuum-solid surface. Since surface effects are restricted to a surface layer on the order of several angstroms, these effects can be described by the differential surface excitation parameter (DSEP) which is the integration of the surface term in the DIIMFP. Including surface effects into the quantitative analysis, background removal in XPS, photoelectron angular distribution, and determination of IMFP from elastic peak electron spectroscopy (EPES) have been investigated.

2. INELASTIC INTERACTIONS IN SOLID SURFACES

We have recently derived the spatially varying DIIMFP of an electron penetrating into vacuum from a solid for quantitative analysis of XPS [10,11]. Here we presented the general formula that include the incoming (IN) and outgoing (OUT) trajectories The notation $v = |v|$, $q = (Q, q_z)$, $v = (v_{||}, v_z)$, and $r = (R, z)$, where Q, $v_{||}$, and R represent components parallel with the interface, will be adopted hereafter.

The vacuum-solid system is the typical case in REELS experiment. Here the solid is considered to be contained in the region $z < 0$. With the dielectric theory, the DIIMFP can be split into a bulk and a surface term. For an electron of energy $E = v^2/2$ to lose energy ω, the spatially varying differential inverse inelastic mean free path (DIIMFP), $\mu(E \to E - \omega, \alpha, z)$, for the IN and OUT trajectories in the vacuum-solid system can be respectively expressed as

$$\mu^{IN}(E \to E-\omega, \alpha', z) = \mu_B(E \to E-\omega) + \mu_S^{IN}(E \to E-\omega, \alpha', z) \quad (1)$$

and

$$\mu^{OUT}(E\to E-\omega,\alpha,z) = \mu_B(E\to E-\omega)+\mu_S^{OUT}(E\to E-\omega,\alpha,z), \quad (2)$$

where

$$\mu_B(E\to E-\omega)=\frac{1}{\pi^2 v}\left\{\int d^2Q\frac{|v_z|}{\tilde{\omega}^2+(v_zQ)^2}\times \mathrm{Im}\left[-\frac{\Theta(-z)}{\varepsilon(\tilde{q},\omega)}\right]\right\}, \quad (3)$$

$$\mu_S^{IN}(E\to E-\omega,\alpha',z)=\frac{1}{\pi^2 v}\int d^2Q \times\frac{|v_z|}{\tilde{\omega}^2+(v_zQ)^2}\mathrm{Im}\left[\Pi_S^{IN}(v,z,Q,\omega)\right] \quad (4)$$

and

$$\mu_S^{OUT}(E\to E-\omega,\alpha,z)=\frac{1}{\pi^2 v}\int d^2Q \times\frac{|v_z|}{\tilde{\omega}^2+(v_zQ)^2}\mathrm{Im}\left[\Pi_S^{OUT}(v,z,Q,\omega)\right], \quad (5)$$

where

$$\Pi_S^{IN}(v,z,Q,\omega) = e^{-Q|z|}\left[\frac{\bar{\varepsilon}(Q,\omega)}{\varepsilon(\tilde{q},\omega)}\frac{\varepsilon(\tilde{q},\omega)-1}{\bar{\varepsilon}(Q,\omega)+1}\right] \times\left[e^{-Q|z|}\Theta(z)-\frac{\left(2\cos(\tilde{\omega}z/v_z)-e^{-Q|z|}\right)\Theta(-z)}{\bar{\varepsilon}(z,Q,\omega)}\right], \quad (6)$$

and

$$\Pi_S^{OUT}(v,z,Q,\omega) = e^{-Q|z|}\left[\frac{\bar{\varepsilon}(Q,\omega)}{\varepsilon(\tilde{q},\omega)}\frac{\varepsilon(\tilde{q},\omega)-1}{\bar{\varepsilon}(Q,\omega)+1}\right] \times\left[\left(2\cos(\tilde{\omega}z/v_z)-e^{-Q|z|}\right)\Theta(z)-\frac{e^{-Q|z|}\Theta(-z)}{\bar{\varepsilon}(z,Q,\omega)}\right]. \quad (7)$$

Here $\tilde{\omega}=\omega-v_{||}\cdot Q$; $\tilde{q}^2=Q^2+\tilde{\omega}^2/v_z^2$; $\Theta(z)$ is the Heaviside step function; α is the angle between the electron velocity and positive z-axis; $\alpha'=\pi-\alpha$ is the angle between the electron velocity and negative z axis. The bulk term $\mu_B(E\to E-\omega)$ which is independent of the position and emission angle gives rise to the well known expression of the DIIMFP of electrons moving in an infinite medium [12]. On the other hand, the surface term is not confined to the interior of the solid, but also takes place, while the electron is at some distance outside the surface.

The energy and momentum conservation can be included by limiting the range of integration over Q as follows:

$$q_-^2\le(\tilde{\omega}/v_z)^2+Q^2\le q_+^2, \quad (8)$$

where $q_\pm=\sqrt{2E}\pm\sqrt{2(E-\omega)}$.

The inverse inelastic mean free paths (IIMFPs) for the IN and OUT trajectories in REELS are then given by

$$\mu^{IN,OUT}(E,\alpha',z) = \int_0^E d\omega\,\mu^{IN,OUT}(E\to E-\omega,\alpha',z). \quad (9)$$

The model dielectric function developed in previous work is used to investigate the inelastic electron interaction near a solid surface., i.e., [10, 11]

$$\varepsilon(q,\omega)=\varepsilon_b-\sum_j\frac{A_j}{\omega^2-\left(\omega_j+q^2/2\right)^2+i\omega\gamma_j} \quad (10)$$

where ε_b is the background dielectric constant due to the effect of polarizable ion cores and A_j, γ_j and ω_j are, respectively, the oscillator strength, damping coefficient, and excitation energy, all associated with the jth oscillator.

Although the IIMFP depends on electron direction and distance from the surface, the angular dependence is indeed rather weak. Therefore, the results presented here are for the case of an electron moving in the direction perpendicular to the surface. Figures 1 (a) and (b) show the position dependence of the IIMFPs in Ni for the IN and OUT trajectories calculated with the model dielectric function. The results show that IIMFPs at the vacuum side in both IN and OUT trajectories decay to zero at a distance on the order of several Ångström. It can be seen that the effective region of the surface excitations at the vacuum side in the IN trajectory is certainly narrower than that in OUT trajectory. This asymmetric phenomenon arise from the different

position dependence of DIMFP in the IN and OUT trajectories. In view of Eqs. (6) and (7), the position factors of the surface effects at the vacuum side are $e^{-Q|z|}\left[2\cos(\omega z/v_z)-e^{-Q|z|}\right]$ and $e^{-2Q|z|}$ for the OUT and IN trajectories, respectively. On the contrary, the effective region of the surface excitations inside the solid in the IN trajectory is obviously wider than that in OUT trajectory due to the opposite dependence.

Since there is the $e^{-Q|z|}$ term in $\Pi_S^{IN}(v,z,Q,\omega)$ and $\Pi_S^{OUT}(v,z,Q,\omega)$, the surface effects have a rather limited extent about the surface [10, 11]. Therefore, surface effects can be practically characterized by the differential surface excitation parameter (DSEP) that is calculated via integration of Eq. (9),i.e.

$$P_S^{IN,OUT}(E\to E-\omega,\alpha) = \int_{-\infty}^{\infty}\frac{dz}{\cos\alpha}\mu_S^{IN,OUT}(E\to E-\omega,\alpha,z), \quad (11)$$

Even though the interval of the integration in Eq. (11) is infinite, the effective contribution is restricted to a limited region extending on both sides of the vacuum-solid surface. In other words, the DSEP includes the total surface effects for an electron penetrating through the effective region of surface excitations, which is around several Ångström.

With the model dielectric function, we calculated the DSEP. Figure 2 depicts the energy loss dependence of the DSEP for a 500 eV electron moving in the direction perpendicular to the Ni surface. It is seen that the DSEP in the OUT trajectory is slightly larger than that in IN trajectory. Even so, the structures and peak positions of DSEP in the IN trajectory are similar to that in the OUT trajectory. It can be also found that surface excitations contribute largely at small energy losses as compared to the bulk excitations.

The surface excitation parameter (SEP) for an electron penetrating a vacuum-solid surface is then given by [10-14]

$$P_S^{IN,OUT}(E,\alpha) = \int_0^E P_S^{IN,OUT}(E\to E-\omega,\alpha)d\omega, \quad (12)$$

The SEP is the probability for a single loss event. The probability of n successive surface plasmons excited by an electron traversing the effective region should obey the Poisson stochastic process:

$$P_n^{IN,OUT} = \frac{1}{n!}\left[P_S^{IN,OUT}(E,\alpha)\right]^n \times\exp\left[-P_S^{IN,OUT}(E,\alpha)\right], \quad (13)$$

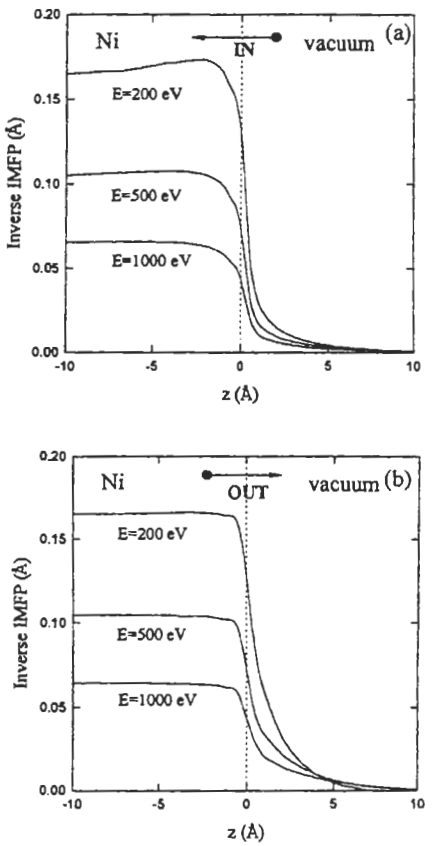

Fig. 1 (a) and (b) Plots of the position dependence of the IIMFPs in Ni for the IN and OUT trajectories calculated with the model dielectric function.

Using the free-electron-gas dielectric function and carrying out the integration in Eq. (13), we found

$$P_S^{IN}(E,\alpha)=P_S^{OUT}(E,\alpha)=\frac{\pi}{4\sqrt{2E}}\frac{1}{\cos\alpha}. \quad (14)$$

It shows that the SEP is proportional to $(\cos\alpha)^{-1}$. Eq. (14) indicates that the influence of surface excitations on surface electron spectroscopies might be quite significant for low-energy electrons at large escape angles. This angular dependence

has been verified experimentally for large α value (~ 85°) [15].

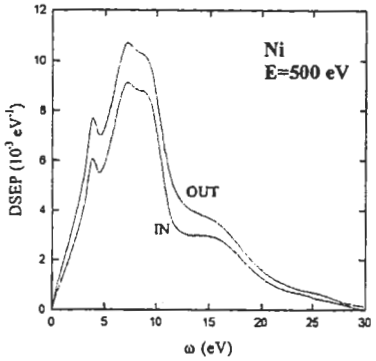

Fig. 2 A plot the energy loss dependence of the DSEP for a 500 eV electron moving in the direction perpendicular to the Ni surface.

Figure 3 shows the SEP calculated with the model dielectric function for an electron moving in the direction perpendicular to the Ni surface. The calculated results show that the electron-energy dependence of the DSEP is rather close to the prediction of the free-electron-gas model derived in Eq. (14). Besides, the SEP in the OUT trajectory is slightly larger than that in IN trajectory, as it may be appreciated in the results of Fig. 2.

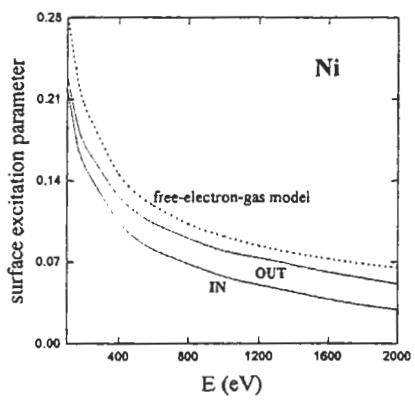

Fig. 3 A plot of the SEP calculated with the model dielectric function for an electron moving in the direction perpendicular to the Ni surface.

3. BACKGROUND REMOVAL

We inputted the calculated DIIMFP and DSEP into the previous formula to evaluate the primary XPS spectra [10]. The direction of x-rays, the direction towards the analyzer and the surface normal are situated in one plane. Figs. 4 and 5 show the primary excitation spectra of Au 4d and Au 4f (solid curves) determined from the experimental Al $K\alpha$-excited photoelectron spectra (dashed curves) [16]. Here we take $\alpha = 15°$ and $\theta = 20°$ for calculations based on the geometry of the VG CLAM 100 analyzer. For comparison, we plot also the corresponding results given by Tougaard (chain curves) [16] who neglected surface excitations. It is found that essentially all intensity far away from a peak is consistently removed. In all case studied the present results are markedly different from the Tougaard's results which consist of a tail extending ~50 eV below the peak. It is seen that the large tail can be almost removed when the surface excitations are considered. Therefore, the large tail occurred in the Tougaard's results is not part of the primary excitation spectrum but may be due to inelastically scattered electrons caused by surface effects.

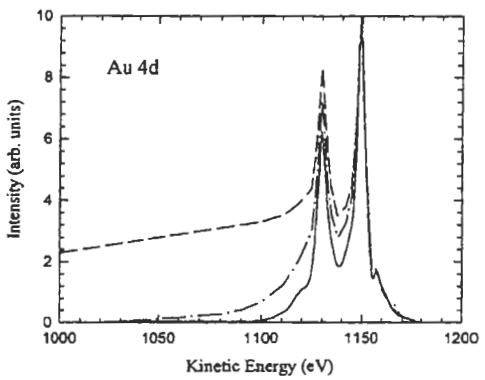

Fig. 4 The primary excitation spectra of Au 4d determined from the Al $K\alpha$-excited photoelectron spectra (dashed curves) [16]. The chain curve is the result of Tougaard [16]

The solid curves in Figs. 4 and 5 still accompany tiny tails. With respect to solid state effect, Penn [17] has pointed out that the intrinsic plasmon loss leads to another shake off. Doniach and Sunjic [18] has also suggested that a single electron excitation induces a shake off process for metals called the Doniach-Sunjic process. Recently, Yoshikawa et al [6] have also found similar satellite peaks in Au 4f source function by using the DIMFP derived from REELS spectrum. They suggests these satellite peaks might correspond to shake-up peaks assoctated with intra-atomic transition. Nevertheless, more complete investigations are necessary to fully account for the tiny tails.

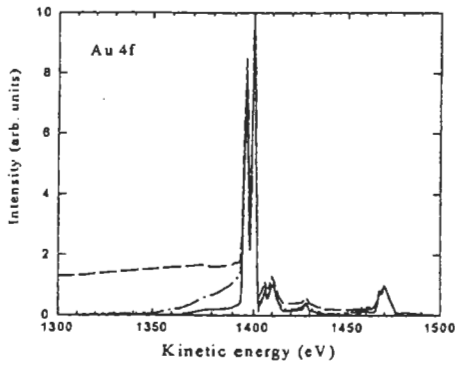

Fig. 5 The primary excitation spectra of Au 4f (solid curve) determined from the experimental Al $K\alpha$-excited photoelectron spectra (dashed curve) [16].The chain curve is the result of Tougaard [16].

4. PHOTOELECTRON ANGULAR DISTRIBUTION

The Monte Carlo method is used to simulate the angular distribution of photoelectrons by recording their trajectories and exit directions. A schematic outline for the considered XPS configuration is shown in Fig. 6. The angle between x rays and the direction of analysis ϕ and the angle α are related by $\phi = 180° - \alpha$. Applying the calculated EDCSs and IMFPs into the Monte Carlo code, we have computed the angular distribution for the electron lines of Au $4p_{3/2}$, Ag $3p_{3/2}$, and Cu $2p_{3/2}$ excited by Al/$K\alpha$ radiation. Figures 7(a)-7(c) show these angular distributions computed with (solid circles) and without (open circles) surface effects. It is seen that surface effects lead to a reduction of the intensities. Comparison with the intensities expected from the straight line approximation (dotted lines) in which elastic scattering and surface effects are neglected shows that the anisotropy in the angular dependence of the photoelectron intensities is always decreased by elastic scattering for $-60° < \alpha < 60°$. On the other hand, the sharp decrease of the photoelectron intensities at large angles is due to the fact that the surface excitation is most probable for glancing electrons, as expected in Eq. (13).

Recently, Jablonski and Zemek [19] have proposed a convenient experimental method for determining the relative angular distribution of photoemission from solid materials. They measured *the ratio* of two different photoelectron intensities at each detection angle to avoid errors associated with determination of the actual analyzed area. Figure 8 compares the experimentally determined ratios of Au 4s and Au 4f intensities with the ratios resulting from the straight line approximation (dotted lines) and the ratios obtained from the Monte Carlo calculations (solid circles). For comparison, we also plot the results computed without surface effects (open circles) in the same figure. Note that all results are normalized so that they are identical at the magic angle ($\alpha = 54°44'$). It is seen that the present results taking into account both surface effects and the elastic scattering of photoelectrons in the solid exhibits a better agreement with experimental data. It can be also seen that the difference between the results computed with and without surface effects nearly vanished in the range of $-60° < \alpha < 60°$ since the surface effects are almost canceled by the ratio. This may be the reason why the previous Monte Carlo results without including surface effects compares well with the experimental data on the ratio of two different photoelectron angular distributions [19,20]. Nevertheless, the influence of surface excitations is still significant at larger detection angles due to the increased surface excitation probability at these angles.

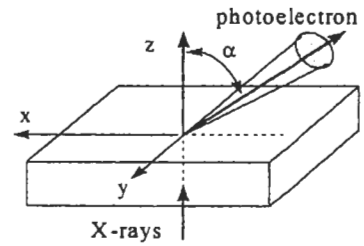

Fig. 6 A schematic outline for the considered XPS configuration

At small detection angles the experimental ratios of photoelectron intensities still deviate from the results of Monte Carlo calculations including surface effects, although to a much smaller extent. These deviations are rather difficult to explain because of the lack of sufficient experimental data. One possible explanation for these deviations is that the interaction of photoelectrons with the positive core hole is completely neglected in the present simulation. However, the deviations can apparently not be accounted for by this interaction process. Therefore, more complete investigations and experiments are necessary in the future to develop a reliable theory of photoelectron transport in solids.

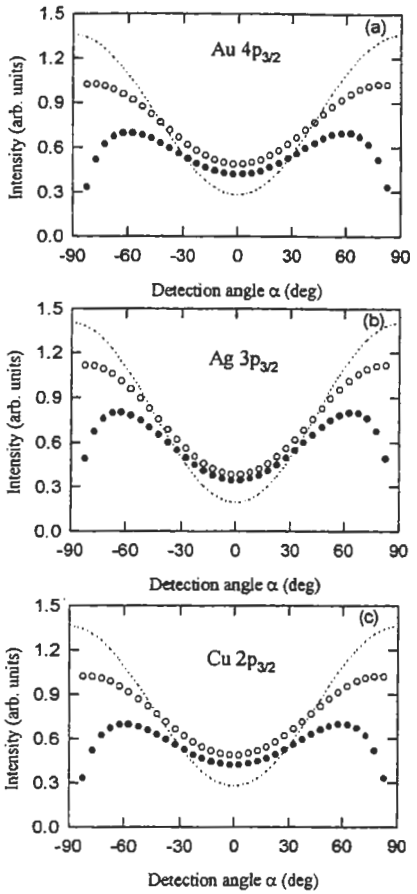

Fig. 7 Dependence of the photoelectron intensity on the detection angle for (a) Au $4p_{3/2}$, (b) Ag $3p_{3/2}$, and (c) Cu $2p_{3/2}$ photoelectrons. Solid circles: Monte Carlo calculations with surface effects; Open circles: Monte Carlo calculations without surface effects; dotted lines: the straight line approximation.

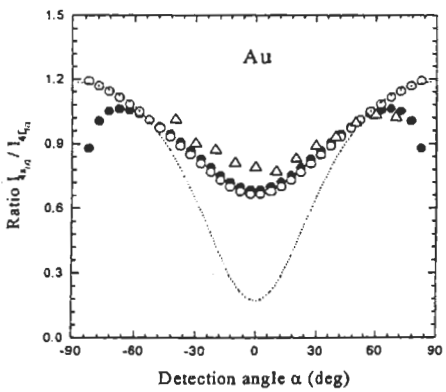

Fig. 8 A plot of ratios of Au 4s and Au 4f photoelectron intensities: Solid circles: Monte Carlo calculations with surface effects; Open circles: Monte Carlo calculations without surface effects; dotted lines: the straight line approximation.; open triangles: experimental data (Ref. [19])

5. References

[1] S. Tougaard and I. Chorkendorff, Phys. Rev. B **35**, 6570 (1987).
[2] S. Tougaard, Surf. Interface. Anal. **11**, 453 (1988).
[3] S. Tougaard and J. Kraaer, Phys. Rev. B **43**, 1651 (1991).
[4] F. Yubero and S. Tougaard, Phys. Rev. B **46**, 2486 (1992).
[5] Z. J. Ding, Phys. Rev. B **55**, 9999 (1997).
[6] H. Yoskikawa, Y. Irokawa, and R. Shimizu, J. Vac. Sci. Technol. A **13**, 1984 (1995).
[7] T. Nagotomi, Z. J. Ding, R. Shimizu, Surf. Sci. **359**, 163 (1996).
[8] J. A. D. Matthew and P. R. Underhill, J. Electron Spectrosc. **14**, 371 (1978).
[9] V. M. Dwyer and J. A. D. Matthew, Surf. Sci. **193**, 549 (1988).
[10] Y. F. Chen and Y. T. Chen, Phys. Rev. B **53**, 4709 (1996).
[11] Y. F. Chen and C. M. Kwei, Surf. Sci. **364**, 131 (1996).
[12] R. H. Ritchie, Phys. Rev. **106**, 874 (1957).
[13] Y. F. Chen, J. Vac. Sci. Technol. A **13**, 2665 (1995)
[14] Y. F. Chen, Surf. Sci. **345**, 213 (1996).
[15] H. Raether, in Excitations of Plasmons and Interband Transitions by Electrons, Ed. G. Hö hler, Springer Tracts in Modern Physics Vol. **88** (Springer, New York, 1980)
[16] S. Tougaard, Phys. Rev. B **34**, 6779 (1986).
[17] D. R. Penn, Phys. Rev. Lett. **38**, 1429 (1977)
[18] S. Doniach and M. Sunjic, J. Phys. C **3**, 285 (1970)
[19] A. Jablonski and J. Zemek, Phys. Rev. B **48**, 4799 (1993).
[20] O. A. Baschenko, G. V. Machavariani, and V. I. Nefedov, J. Electron. Spectrosc. Relat. Phenom. **34**, 305 (1984).